Supporting Information

Synergistic Photothermal Conversion and Photocatalysis in 2D/2D MXene/Bi_2S_3 Hybrids for Efficient Solar-Driven Water Purification

*Yang Liu [a], Shu-Zhou Qu [a], Ze-Run Zhou [a], Xiang-Ping Song [c], Liang Ma [a] *, Si-Jing Ding [b], Qu-Quan Wang [d]**

[a] Hubei Key Laboratory of Optical Information and Pattern Recognition, Wuhan Institute of Technology, Wuhan, 430205, P. R. China.

[b] School of Mathematics and Physics, China University of Geosciences (Wuhan), Wuhan, 430074, P. R. China.

[c] Department of Pharmacology, Xiangya School of Pharmaceutical Sciences, Central South University, Changsha, 410078, China

[d] School of Science, Department of Physics, Southern University of Science and Technology, Shenzhen, 518055, P. R. China.

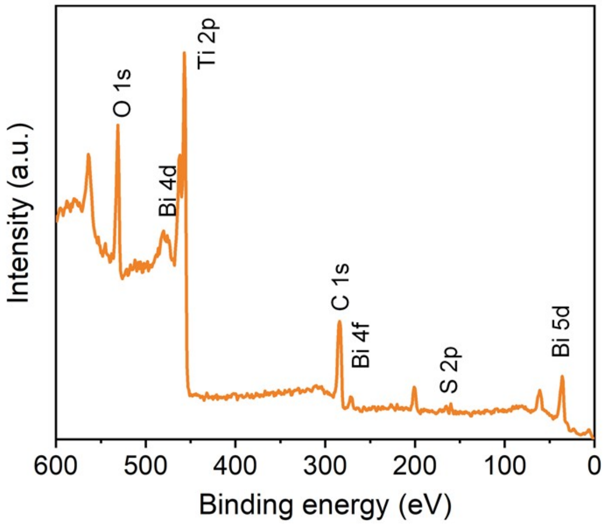

Figure S1. XPS survey of MXene/Bi_2S_3 hybrids.

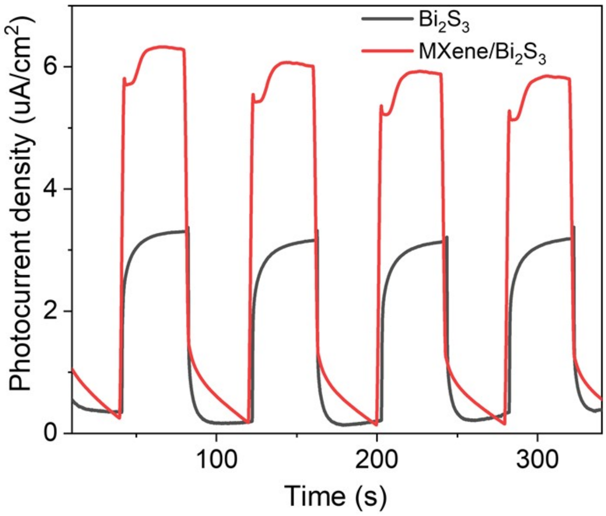

Figure S2. Photocurrent densities of Bi_2S_3 and MXene/Bi_2S_3 electrodes under light irradiation. In the measurements, Pt electrode and AgCl electrode were used as counter electrode and reference electrode, Na_2SO_4 (1 M) was used as electrolyte.

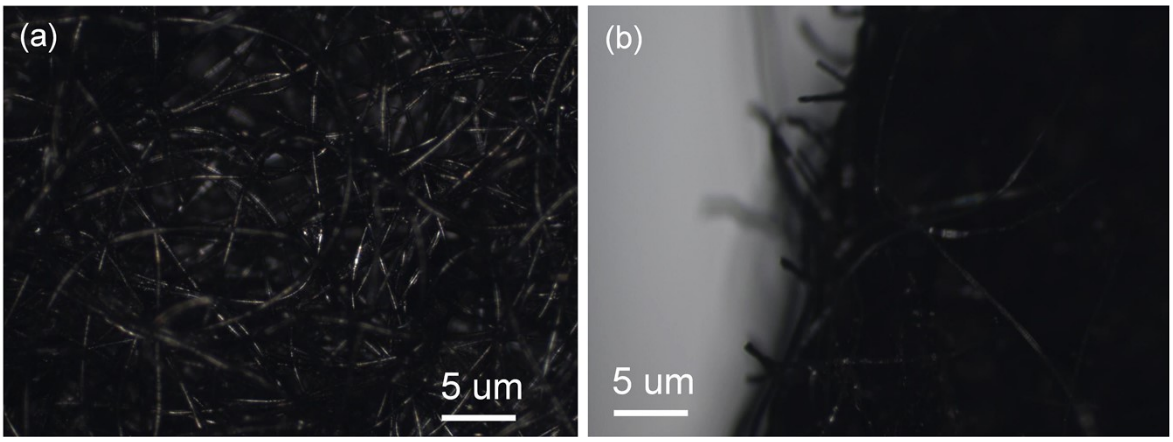

Figure S3. Optical images of MXene/Bi_2S_3 hybrids observed on top view (a) and side view (b).

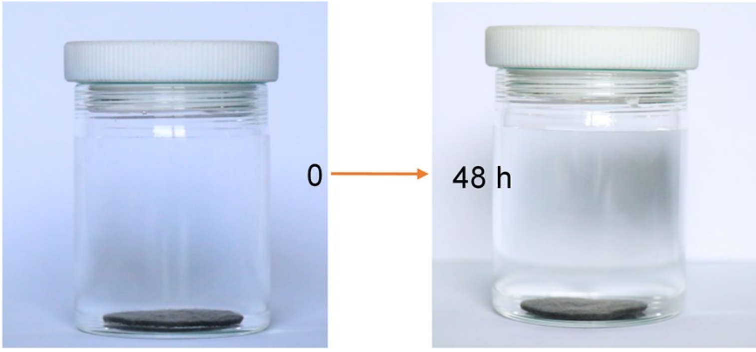

Figure S4. Photographs of MXene/Bi_2S_3 membrane soaking in water for 48 h.

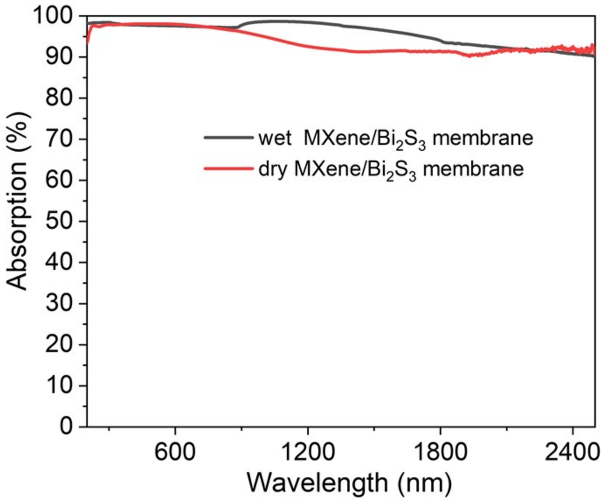

Figure S5. Absorption spectra of wet and dry MXene/Bi_2S_3 membranes.

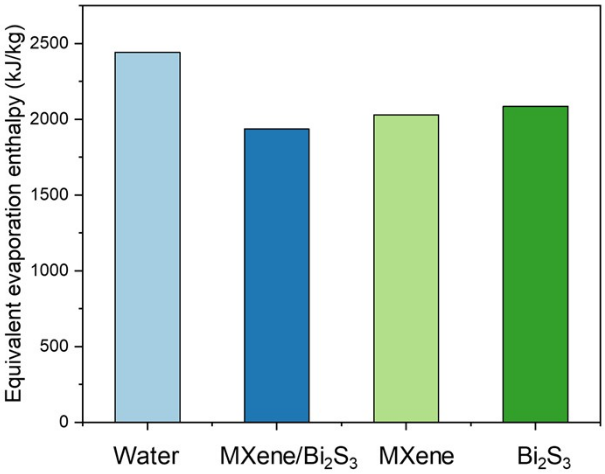

Figure S6. Equivalent vaporization enthalpy of Bi_2S_3, MXene, and MXene/Bi_2S_3 membranes. The calculation is based on the formula $\Delta H_0 \mathrm{m}_0 = \Delta H_{equ} m_g$, where ΔH_0 is the evaporation enthalpy of pure water, m_0 is the spontaneous evaporation rate of water in dark, m_g is spontaneous evaporation rate of membrane, ΔH_{equ} is the equivalent vaporization enthalpy.

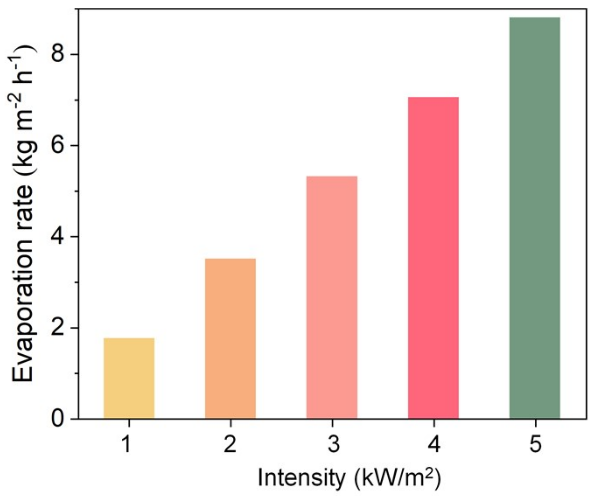

Figure S7. Mass change of water in the presence of MXene/Bi_2S_3 membrane under sunlight irradiation with different intensities.

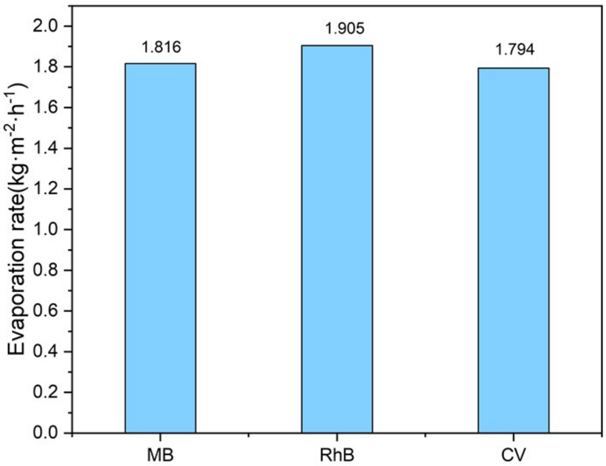

Figure S8. Evaporation rates of MXene/Bi_2S_3 membrane measured in MB, RhB, and CV solution.

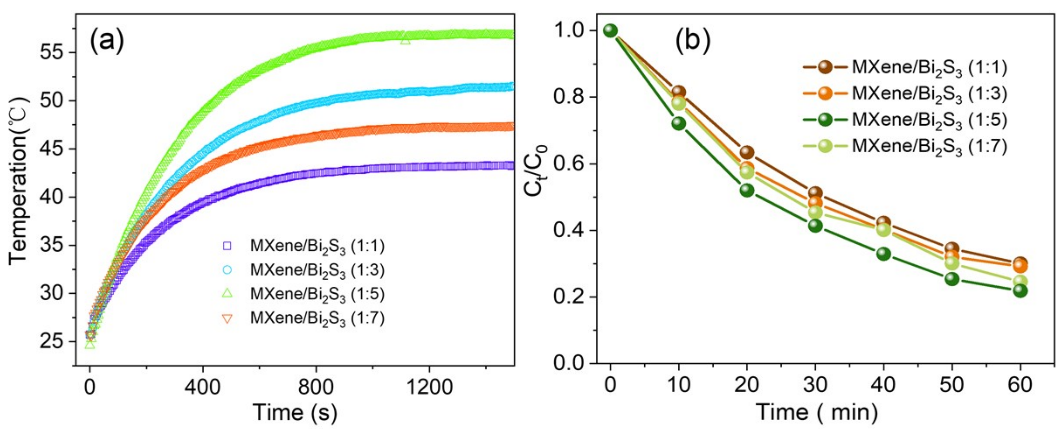

Figure S9. Temperature variation curves (a) under an 808 nm laser irradiation and photocatalytic degradation of MB (b) in the presences of MXene/Bi_2S_3 with different mass ratios.

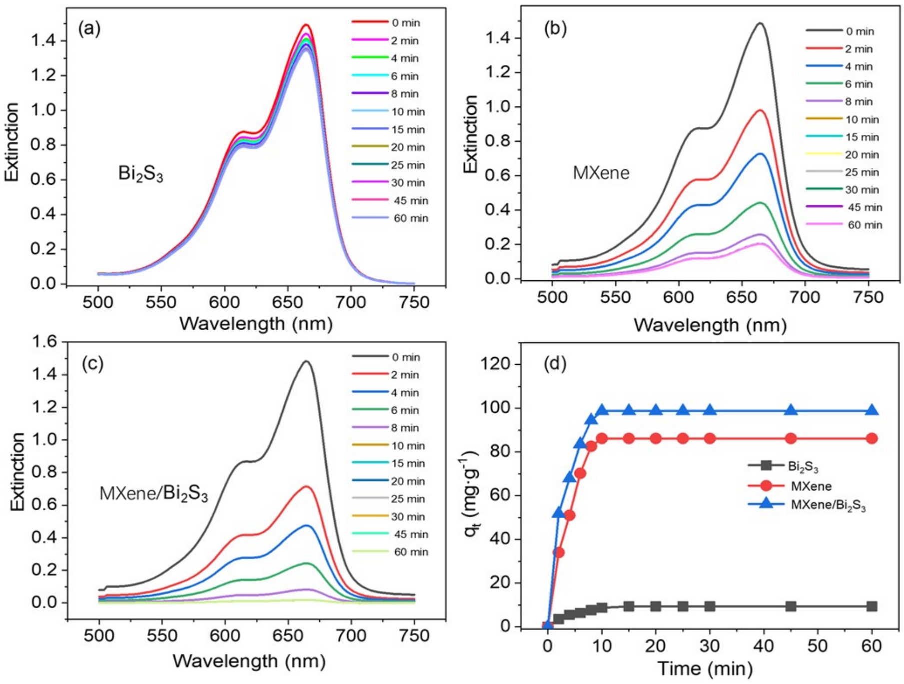

Figure S10. Time-dependent extinction spectra of MB in the presences of Bi_2S_3 (a), MXene (b), and MXene/Bi_2S_3 (c). (d) The comparison of adsorption abilities of Bi_2S_3, MXene, and MXene/Bi_2S_3.

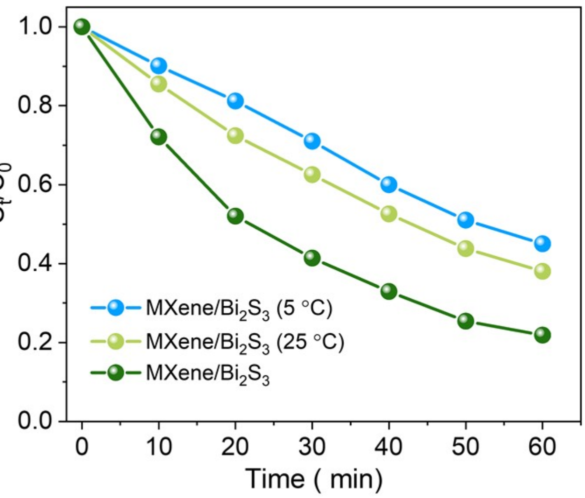

Figure S11. The photocatalytic degradation of MB of MXene/Bi_2S_3 measured at different temperature controlled by cooling water.

Table S1. Comparison of the photothermal conversion efficiency (PCE) of some typical hybrids reported in previous work.

Materials	Excitation wavelength	PCE	Reference
MXene/Bi_2S_3	808 nm	45.1%	This work
Au@Bi_2S_3	808 nm	35.3%	31
$Cu_{1.94}S/Bi_2S_3$	808 nm	33.2%	32
$Bi_2S_3/Cu_2S/Cu_3BiS_3$	808 nm	43.8%	33
BiOI@Bi_2S_3	808 nm	28.5%	34
Bi_2S_3/FeS_2	808 nm	38.7%	35

Table S2. Comparison of the evaporation rate of some typical membranes.

Materials	Solar vapor generation (kg m^{-2} h^{-1})	Reference
MXene/Bi_2S_3	1.77	This work
MXene/CuInSe	1.43	36
MXene/Cu_3BiS_3	1.32	37
Pd-Bi_2S_3	1.61	38
Borophene/CNF	1.45	39
Au@Bi_2MoO_6-CDs	1.69	40
MXene/rGO	1.33	41